ARTICLE

Facile Green Synthesis of Magnetic Fe_3C@C Nanocomposite using Natural Magnetite

Ju-wen Gu, Yong Bai, Song-bai Qiu*, Qian Zhang, Tie-jun Wang*

School of Chemical Engineering and Light Industry, Guangdong University of Technology, Guangzhou 510006, China

(Dated: Received on July 23, 2019; Accepted on September 10, 2019)

One simple and environmental friendly synthesis strategy for preparing low-cost magnetic Fe_3C@C materials has been facilely developed using a modified sol-gel approach, wherein natural magnetite acted as the iron source. A chelating polycarboxylic acid such as citric acid (CA) was employed as the carbon source, and it dissolved Fe very effectively, Fe_3O_4 and natural magnetite to composite an iron-citrate complex with the assistance of ammonium hydroxide. The core-shell structure of the as-prepared nanocomposites was formed directly by high-temperature pyrolysis. The Fe_3C@C materials exhibited superparamagnetic properties (38.09 emu/mg), suggesting potential applications in biomedicine, environment, absorption, catalysis, *etc.*

Key words: Magnetic material, Natural magnetite, Fe_3C@C, Citric acid complexation

I. INTRODUCTION

Recently, magnetic nanomaterials have attracted extensive attention of both the research and industrial communities in the magnetic electronic, optical, environmental, catalytic, medical, and chemical properties [1−4]. Especially, iron carbide (Fe_3C) nanoparticles exhibit potential applications due to the excellent saturation magnetization and low toxicity. Several methods have been reported to synthesize Fe_3C nanomaterials such as magnetron sputtering, laser pyrolysis, chemical vapor deposition and high-temperature pyrolysis [3−8]. Considering cost-effect and scalableness, Fe_3C based materials are commonly prepared by pyrolysis of C-containing precursors in the presence of Fe salts [3−8]. In human society, iron is the most common and most widely used one among all the metal, accounting for 95% of worldwide metal production. All kinds of metallic iron and iron salts must be originated from the ironmaking industry by smelting various iron ores such as hematite (Fe_2O_3), magnetite (Fe_3O_4), and siderite ($FeCO_3$), *etc.* The application of natural iron minerals as iron precursors is attractive due to their wide availability and low cost [1, 9].

In this work, natural magnetite was selected as the iron source, just as iron metal and ferroferric oxide, for preparing the magnetic Fe_3C@C nanomaterials by modified sol-gel method. Citric acid was used as a multidentate ligand and it dissolved iron from natural magnetite very effectively through coordination [10]. In the process of dissolution, it was important for the base to be employed in an amount sufficient to adjust the pH of the solution in the range of 3−4. When ammonia was admixed with citric acid, the formed ammonium citrate could react with the iron element to form an iron-citrate complex, leading to the occurrence of faster dissolution and high solubility. Ultimately, the Fe_3C nanoparticles embedded in the carbon layers were obtained after the ligand was removed by thermal decomposition of the fully dried gel.

II. EXPERIMENTS

A. Synthesis of Fe_3C@C material

The Fe_3C@C materials were synthesized by pyrolysis using a modified sol-gel approach. A proper amount of Fe_3O_4 (AR), natural magnetite or iron powder (AR), and citric acid (AR) were mixed in deionized water, and then the pH value of the solution was adjusted to 3−4 by the addition of ammonia (AR). The total iron grade of natural magnetite was 62.55 wt%, the FeO content was 25.30 wt%, and other chemical compositions mainly contained SiO_2 3.20 wt%, Al_2O_3 0.59 wt%, CaO 1.50 wt%, MgO 3.04 wt%, K_2O 0.054 wt%, Na_2O 0.026 wt%, TiO_2 0.041 wt%, P 0.017 wt%, S 2.94 wt%, Cu 0.11 wt%. The molar ratio of Fe to citric acid was 1:3, and the weight of natural magnetite equaled that of Fe_3O_4. Iron element in Fe_3O_4, iron powder and natural magnetite were effectively dissolved to form an iron-citrate complex. Subsequently, the mixture gelled gradually by evaporation at 100 °C for several days until the gel dried thoroughly. Finally, the fully dried gel

*Authors to whom correspondence should be addressed. E-mail: qiusb@gdut.edu.cn, tjwang@gdut.edu.cn

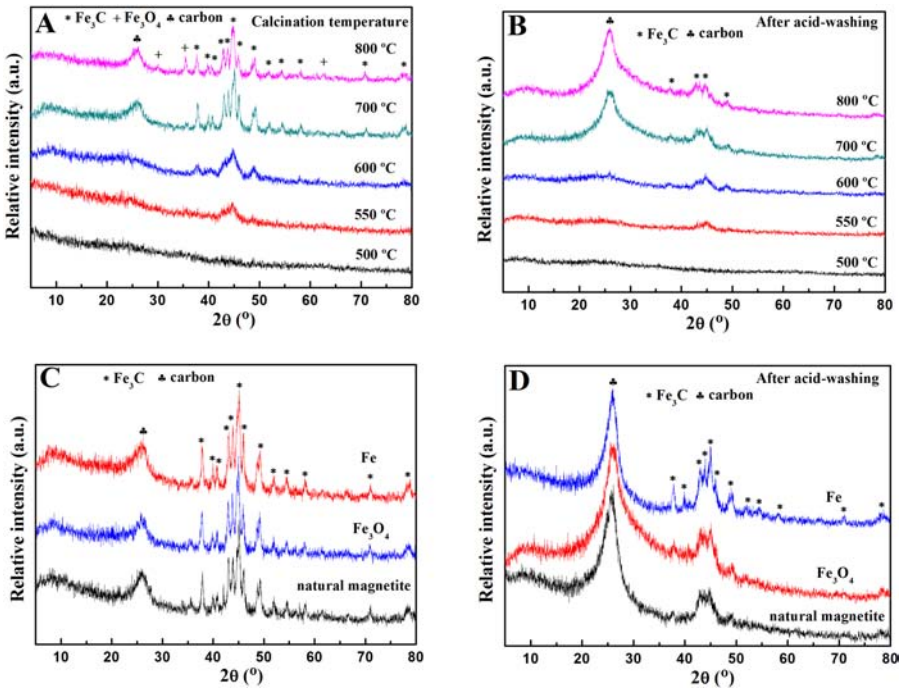

FIG. 1 XRD patterns of the Fe_3C@C samples from (A) Fe_3O_4 and (B) after acid-treatment, and (C, D) from different iron sources with (D) after acid-treatment calcined at 700 °C.

was carbonized at 500−900 °C for 2 h with heating rate of 10 °C/min in N_2. For comparison, the solid products were washed five times with 10.0 wt% H_2SO_4 at 85 °C for 12 h to remove unwrapped iron, and subsequently the residues were washed with de-ionized water.

B. Catalyst characterizations

X-ray diffraction (XRD) patterns were recorded by Rigaku SmartLab (3 KW, Japan) with Cu Kα radiation (λ=0.154 nm, Philip) operated at 40 kV and 30 mA. Scanning electron microscopy (SEM) using FEI Quanta 400 FEG (America) and transmission electron microscopy (TEM) using Talos F200S (Czech Republic) were used to study the textural properties and morphologies of the samples. Elemental analysis for the samples was carried out using inductively coupled plasma-optical emission spectroscopy (ICP-OES, Optima 8000, Perkin-Elmer). The magnetic properties of the samples were investigated using a vibrating sample magnetometer (Quantum Design SQUID-VSM) with applied magnetic fields between −20 and 20 kOe at 300 K.

III. RESULTS AND DISCUSSION

A. Characterization of the catalysts

FIG. 1(A) displays the XRD patterns of Fe_3C@C materials that were prepared at different calcination temperatures. The components of the pyrolysis products varied with increasing temperatures from 500 °C to 800 °C. When heated up to 700 °C, the broad reflection at about 26° began to emerge, which was indexed to the (002) plane of graphitic carbon (JCPDS No.41-1487) [11]. These results indicated that the degree of graphitization of the prepared composites depended strongly on calcination temperatures, and higher temperatures could promote the carbonization process. Apart from this reflection, other reflections in 37°−50° were assigned to the typical diffraction of Fe_3C phase (JCPDS No.89-2867) [11], and gradually occurred with increasing the calcination temperature to over 550 °C. The diffraction peaks at around 37.8°, 39.9°, 40.7°, 42.9°, 43.9°, 44.7°, 45.1°, 46.0°, 48.7°, 49.1°, 52.0°, 54.5°, 58.1°, 70.9°, and 78.8°, correspond to (210), (002), (201), (211), (102), (220), (031), (112), (131), (221), (122), (040), (301), (123), and (133) planes of Fe_3C nanoparticles, respectively. Firstly, the intensity of those reflections increased with calcination temperature, and then reached maximum at the temperature region of 700−800 °C, implying that 700 °C was the optimal temperature for nucleation and crystal growth of Fe_3C. Besides, when heated at 800 °C, the very weak peaks at 30.1°, 35.5° and 62.6° confirmed the existence of trace Fe_3O_4 in the pyrolysis products. This could be attributed to a small amount of CO_2 and H_2O derived from the oxygen-containing functional groups of citric acid during the high carbonization process [11].

Moreover, the elemental composition of the Fe_3C@C sample from natural magnetite was analyzed by ICP-OES, including Fe 39.00 wt%, SiO_2 0.73 wt%, Al_2O_3

DOI:10.1063/1674-0068/cjcp1907142

0.13 wt%, CaO 0.12 wt%, MgO 0.65 wt%, K_2O 0.0059 wt%, Na_2O 0.020 wt%, TiO_2 0.021 wt%, P 0.00079 wt%, S 0.32 wt%, Cu 0.0078 wt%. Based on the elemental compositions of the relative precursor and pyrolysis product, the iron element in the natural magnetite could be selectively dissolved by means of coordination effect between Fe and CA. Only a small amount of other mineral elements were dissolved and dispersed into the iron precursors during complexing dissolution. The textural property of the Fe_3C@C sample was investigated using standard BET and BJH theory, respectively. In the case of natural magnetite, the dense structure of natural ores led to a little specific surface area (0.15 m^2/g) and pore volume (0.004 cm^3/g). By contrast, the Fe_3C@C sample derived from natural magnetite was of high special surface area (262.4 m^2/g) and large pore volume (0.25 cm^3/g) due to the formation of a special core-shell structure, which was in line with the following TEM observations.

The heat-treated samples were repeatedly washed with 10.0 wt% H_2SO_4 in order to remove any unprotected iron nanoparticles. The corresponding XRD diffraction patterns of the materials were illustrated in FIG. 1(B). After acid treatment, the intensity of the Fe_3C peaks decreased significantly, but the intensity of the graphite peak increased obviously. The unstable iron species gradually dissolved and disappeared in the acid solution, and the relatively more stable Fe_3C nanoparticles wrapped with the carbon layers were retained. Therefore, this phenomenon showed that the carbon shell derived from the carbonization of citric acid was essential for protecting the magnetic nanoparticles against acid corrosion [12].

As shown in FIG. 1(C, D), this synthetic strategy was also applied with other iron sources such as analytically pure Fe and Fe_3O_4. It was observed that the heat-treated composites at 700 °C also contained magnetic Fe_3C nanoparticles. After acid washing, there only remained the diffraction peaks of Fe_3C except the peak of graphitic carbon at around 26°. Most of these Fe_3C nanoparticles without integral carbon layers were eliminated as a consequence of acid corrosion, which resulted in a high content of residual graphite and the increasing intensity of the carbon peaks. Thus, this synthetic strategy was particularly attractive to produce magnetic components in one special core-shell structure *in situ* carbonization of citric acid using different iron sources [13, 14].

In order to further explore the morphological structure of Fe_3C@C samples obtained at 700 °C, the typical SEM and TEM analyses were conducted, the results are shown in FIG. 2 and FIG. 3, respectively. The SEM images clearly showed that the samples were near-spherical nanoparticles, which exhibited uniform morphologies of the self-assembled aggregate composite. For comparison, the Fe_3C@C sample obtained at 500 °C from Fe_3O_4 was investigated by TEM, and FIG. 3(A) shows the results before and after acid washing. After annealing, clearly visible iron-rich nanoparticles were well-dispersed on the amorphous carbon matrix. For this sample, no well-defined crystalline lattice was observed, suggesting a poor crystalline property, in agreement with the XRD analysis. However, after acid treatment, the iron nanoparticles were removed and disappeared thoroughly, leaving behind apparent honeycomb-like holes on the carbon layer. Consequently, FIG. 3A(b) clearly proved its embedded structure, and the iron nanoparticles were semi-encapsulated by the amorphous carbon layers. According to TEM images in FIG. 3(B, C), the iron nanoparticles agglomerate due to sintering or collapsing and regular lattice fringes presented during treatment at higher temperature. It was clear that the lattice spacing of 0.20 and 0.22 nm matched well with the (031) and (211) planes of Fe_3C, and the lattice spacing of 0.34 nm was assigned to the (002) planes of graphite. Based on the XRD patterns and TEM images, it was confirmed that the samples produced from different iron sources at 700 °C were composed of an outer layer of graphite carbon with a core-shell structure and an Fe_3C core. Moreover, the nanoparticles with a complete and tight encapsulation could have a protective role here against acid corrosion and oxidation. In addition, these results also indicated that the calcination temperatures were critical to the degree of crystallization and the formation of the special core-shell structure.

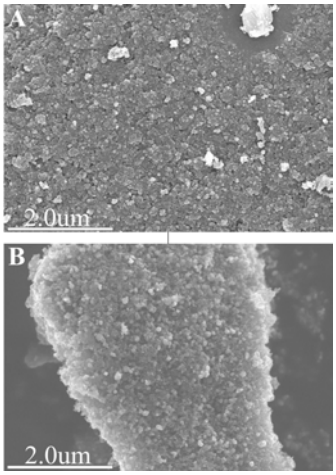

FIG. 2 Typical SEM images of the Fe_3C@C samples obtained at 700 °C from (A) Fe_3O_4 and (B) natural magnetite.

A more detailed investigation of the magnetic properties of the as-prepared nanocomposites was performed at room temperature. As shown in FIG. 4, a characteristic hysteresis loop could be observed, indicating the ferromagnetic character of the samples. As for the different Fe sources such as natural magnetite, Fe_3O_4, and Fe, the corresponding Fe_3C@C materials showed superparamagnetic properties with relatively high saturation magnetization moments 38.09, 39.03, and 36.02 emu/mg at room temperature, respectively. In spite of

DOI:10.1063/1674-0068/cjcp1907142

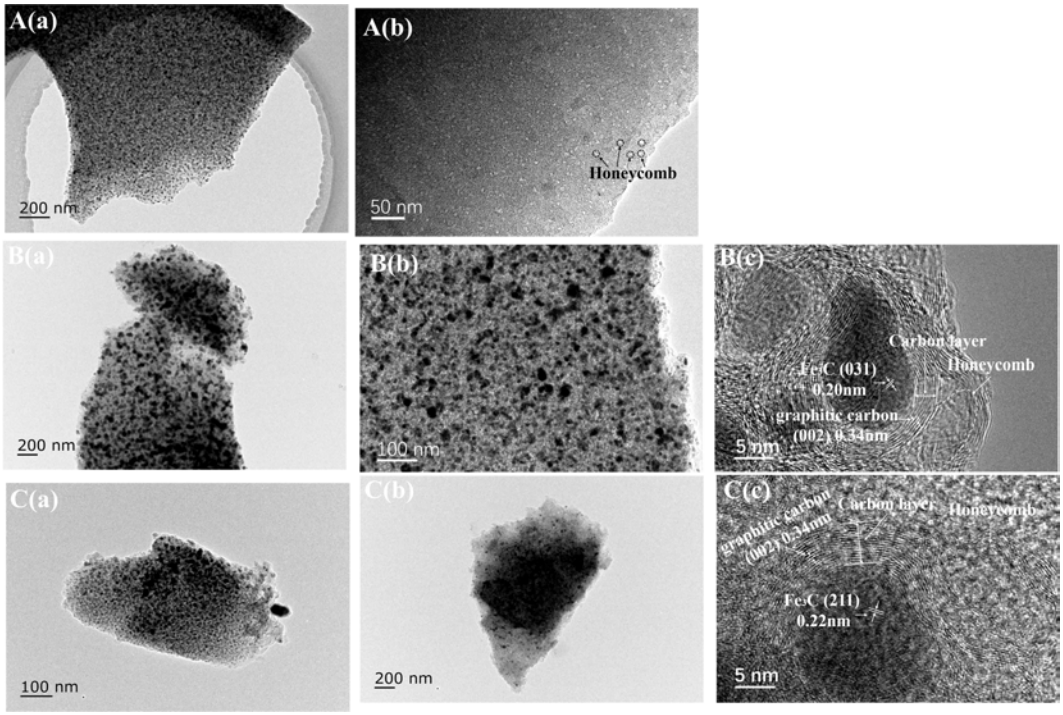

FIG. 3 TEM images of the Fe_3C@C samples obtained at 500 °C from Fe_3O_4 A(a) before and A(b) after acid-treatment, at 700 °C from Fe_3O_4; B(a) before, B(b) and B(c) after acid washing, at 700 °C with natural magnetite; C(a) before, C(b) and C(c) after acid washing.

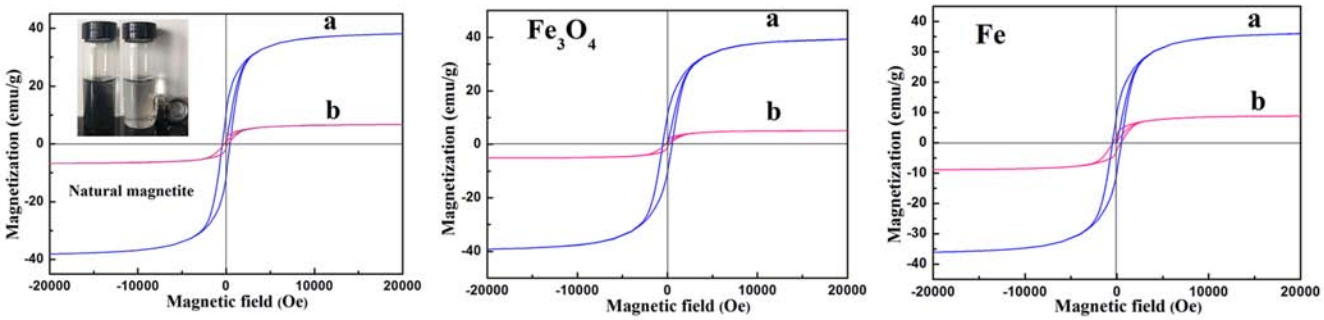

FIG. 4 The magnetic hysteresis loop of the Fe_3C@C samples prepared from different iron sources at 700 °C (a) before and (b) after acid washing.

the acid attack, the relative nanocomposites still held the remarkable residue of the saturation magnetization value around 6.74, 5.11, and 8.81 emu/mg, respectively, which is high enough to enable the sample to be manipulated by conventional magnets. The photographs in the left inset of FIG. 4 proved that the Fe_3C@C nanoparticles dispersed in aqueous solution could be easily harvested and separated by an external magnetic field.

FIG. 5 indicated the schematic of synthesis process of the Fe_3C@C materials by modified sol-gel method. Firstly, the starting materials, water, citric acid and natural magnetite were mixed, and then the pH of the solution was adjusted in the range of 3−4 using ammonia. By amination reaction, the formed ammonium citrate could react more quickly with the iron oxides to form an iron-citrate complex, resulting in the effective dissolution and stable dispersion of the iron precursors ($H_3C_6H_5O_7+NH_4OH\rightarrow NH_4H_2C_6H_5O_7+H_2O$, $3NH_4H_2C_6H_5O_7+Fe_3O_4\rightarrow NH_4FeC_6H_5O_7+2FeC_6H_5O_7+2H_2O+2NH_4OH$). In the drying process, a stabilized homogeneous mixture of brown functional gel gradually formed. Environmentally friendly polycarboxylic acid such as citric acid acted not only as one multidentate coordination agent but also as a carbon source and reductant. During high-temperature pyrolysis, the polymer gel simultaneously decomposed around these iron nanoparticles, producing a carbon-rich matrix. The initial nucleation of iron species could re-crystallize to form a graphitic carbon layer encapsulated Fe_3C

DOI:10.1063/1674-0068/cjcp1907142

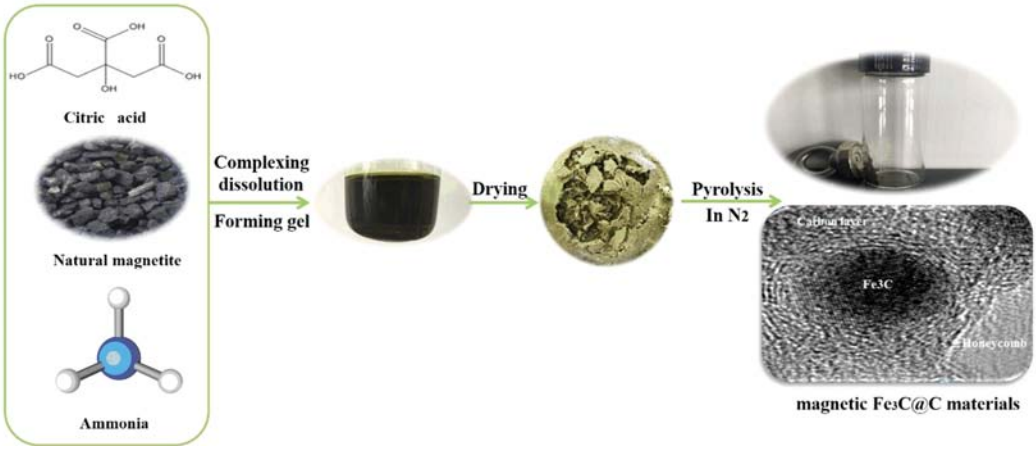

FIG. 5 Schematic of the synthesis process of the Fe_3C@C samples modified by sol-gel method.

nanoparticles with a core-shell structure on further heating [14, 15].

IV. CONCLUSION

In summary, the magnetic Fe_3C@C materials have been facilely and greenly fabricated by modified sol-gel method from natural magnetite. Citric acid not only played a key role in complexing dissolution of iron species as a complexant, but also in formation of a core-shell structure as one carbon source and reductant during the thermal pyrolysis. The calcination temperature was a critical parameter in improving the degree of crystallization and the formation of complete and tight encapsulation. The Fe_3C@C materials showed superparamagnetic properties with a relatively high saturation magnetization moment 38.09 emu/mg at room temperature, and still kept 6.74 emu/mg after acid corrosion due to protection of the integral graphene shell. This simple and environmental friendly synthesis strategy for preparing low-cost magnetic material could find numerous potential applications in future.

V. ACKNOWLEDGMENTS

This work was supported by the National Natural Science Foundation of China (No.51876046 and No.51711540032).

[1] M. Munoz, Z. M. de Pedro, J. A. Casas, and J. J. Rodriguez, Appl. Catal. B **176**, 249 (2015).
[2] Y. Pan, X. W. Du, F. Zhao, and B. Xu, Chem. Soc. Rev. **41**, 2912 (2012).
[3] L. Mohammed, H. G. Gomaa, D. Ragab, and J. Zhu, Particuology **30**, 1 (2017).
[4] J. P. Wang, Y. Z. Chen, S. J. Yuan, G. P. Sheng, and H. Q. Yu, Water Res. **43**, 5267 (2009).
[5] Y. C. Wu, J. R. Rao, and X. F. Li, Chin. J. Chem. Phys. **31**, 576 (2018).
[6] B. Tang, G. X. Hu, and M. Xia, Mater. Lett. **68**, 104 (2012).
[7] S. Atiq, S. M. Ramay, A. Mahmood, S. Riaz, and S. Naseem, Chin. J. Chem. Phys. **29**, 245 (2016).
[8] Z. T. Ye, P. Zhang, X. Lei, X. B. Wang, N. Zhao, and H. Yang, Chem. Eur. J. **24**, 8922 (2018).
[9] F. Y. Gong, T. Q. Ye, L.X. Yuan, T. Kan, Y. Torimoto, M. Yamamoto, and Q. X. Li, Green Chem. **11**, 2001 (2009).
[10] V. R. Ambikadevi and M. Lalithambika, Appl. Clay Sci. **16**, 133 (2000).
[11] X. B. Wang, P. Zhang, J. J. Gao, X. D. Chen, and H. Yang, Dyes Pigment. **112**, 305 (2015).
[12] P. Gorria, M. Sevilla, J. A. Blanco, and A. B. Fuertes, Carbon **44**, 1954 (2006).
[13] J. Bao, J. J. He, Y. Zhang, Y. Yoneyama, and N. Tsubaki, Angew. Chem. Int. Ed. **47**, 353 (2008).
[14] A. V. Erokhin, E. S. Lokteva, A. Y. Yermakov, D. W. Boukhvalov, K. I. Maslakov, E. V. Golubina, and M. A. Uimin, Carbon **74**, 291 (2014).
[15] Y. Hu, J. O. Jensen, W. Zhang, L. N. Cleemann, W. Xing, N. J. Bjerrum, and Q. Li, Angew. Chem. Int. Ed. **53**, 3675 (2014).

DOI:10.1063/1674-0068/cjcp1907142